Int. J. Heat Mass Transfer. Vol. 25, No. 11, pp. 1701–1707, 1982
Printed in Great Britain

0017-9310/82/111701-07 $03.00/0

TEMPERATURE DISTRIBUTION IN AND AROUND A BURIED HEAT GENERATING SPHERE

HAIM H. BAU
Department of Mechanical Engineering and Applied Mechanics, University of Pennsylvania, Philadelphia, PA 19104, U.S.A.

(*Received* 30 *June* 1981 *and in final form* 19 *March* 1982)

Abstract—An exact analytical solution is presented for the steady-state temperature distribution in and around a heat generating sphere buried in a semi-infinite solid with an isothermal surface. This analysis does not require that the thermal conductivities of the medium and the sphere be equal. The exact solution, derived using a bispherical coordinate system, is compared with an approximate source–sink solution. The results include the temperature distribution in and around the sphere, the form factor and the heat flux distribution along the medium surface.

NOMENCLATURE

- a, scale factor for the bispherical coordinates, $\sinh \beta_0$;
- A_n, numerical coefficients in the ϕ_1 series, equation (4);
- C_n, numerical coefficients in the ϕ_2 series, equation (5);
- D, location of the sphere center beneath the surface [m];
- F, form factor;
- g, internal heat generation [$\mathrm{W\,m^{-3}}$];
- k, thermal conductivity [$\mathrm{W\,m^{-1}\,K^{-1}}$];
- n, integer;
- N, number of leading terms used in the infinite series;
- P_ν, Legendre polynomial of the first kind of order ν;
- q, heat flux, nondimensional;
- r, radial (horizontal) rectangular coordinate, $a \sin \alpha/(\cosh \beta - \cos \alpha)$;
- R, the sphere radius [m];
- T, temperature [K];
- z, vertical, rectangular coordinate.

Greek symbols

- α, β, bispherical coordinates (Fig. 1);
- β_0, the sphere surface, $\cosh^{-1}(D/R)$;
- ϕ, temperature, nondimensional.

Superscripts

- $^{\sim}$ source–sink solution.

Subscripts

- 1, values inside the sphere;
- 2, values outside the sphere;
- AV, average.

1. INTRODUCTION

THE DETERMINATION of the temperature distribution in and around a buried heat source is relevant to the solution of many engineering problems such as burial of nuclear waste, storage of nuclear materials and cooling of electrical equipment.

A sphere of radius R and uniform heat generation g is considered. The sphere center is located at depth D beneath the isothermal surface of a semi-infinite medium (Fig. 1). The method of analysis most often used in determining the temperature distribution in and around a buried sphere is based upon the superposition of source and sink solutions [1–3]. The above yields exact results for the special case when the thermal conductivity of the sphere equals that of the semi-infinite medium. When the thermal conductivities differ, however, the source–sink solution may only serve as an approximation, whose accuracy deteriorates as the burial depth (D/R) decreases. The purpose of this paper is to provide an exact solution which will be valid regardless of the sphere burial depth or the ratio of the thermal conductivities and to compare it with the source–sink solution in order to establish when the approximation can be used.

Exact analytical solutions for a buried sphere can be obtained by applying a bispherical coordinate system [4–6]. Such a coordinate system is 'natural' for this problem since the boundary conditions—the sphere and the semi-infinite medium surfaces—are located along a constant value coordinate (Fig. 1). Consequently, the heat conduction equation is separable.

The bispherical coordinate system has been used previously to solve heat transfer problems from an isothermal sphere buried beneath isothermal [4, 8], adiabatic [6, 8], and convecting surfaces [7].

2. ANALYSIS—EXACT SOLUTION

Consider a sphere of radius R, thermal conductivity k_1, and uniform heat generation g, whose center is located at depth D below the surface of a semi-infinite solid (Fig. 1). The surface temperature of the semi-infinite solid is uniform, and its thermal conductivity is k_2. We use R as the length scale and $(gR^2)/k_1$ as the temperature scale. The steady-state, non-dimensional

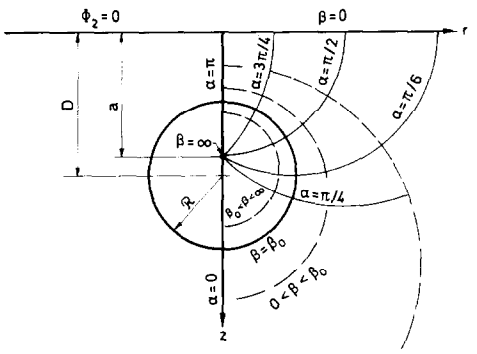

FIG. 1. The bispherical coordinate system.

temperature $\phi_i(r, z)$ can be found by solving the heat equation

$$\nabla^2\phi_i = \begin{cases} -1 & \text{in the sphere } (i = 1). \\ 0 & \text{outside the sphere } (i = 2), \end{cases} \quad (1)$$

where ϕ_1 and ϕ_2 respectively denote temperatures inside and outside the sphere. The above geometry can be described in more convenient form through the use of a bispherical coordinate system. This is achieved by using the mapping [4–6]

$$z + ir = ia\cot[(\alpha + i\beta)/2], \quad 0 \leqslant \alpha \leqslant \pi, \quad -\infty < \beta < \infty \quad (2)$$

where surfaces of α = constant and β = constant appear respectively as orthogonal spindles and spheres (Fig. 1). The sphere surface is $\beta = \beta_0 = \cosh^{-1}(D/R)$ and the scale factor is $a = \sinh\beta_0$. The appropriate boundary conditions are

$$\phi_1 \text{ finite at } \beta \to \infty, \quad (3a)$$

$$\phi_1 = \phi_2 \text{ and } k_1\frac{\partial\phi_1}{\partial\beta} = k_2\frac{\partial\phi_2}{\partial\beta} \quad \text{at } \beta = \beta_0, \quad (3b)$$

$$\phi_2 = 0 \quad \text{at } \beta = 0. \quad (3c)$$

Applying boundary conditions (3a) and (3c), we obtain the following solutions:

$$\phi_1 = -\frac{1}{3}\frac{a^2\cosh\beta}{(\cosh\beta - \cos\alpha)} + (\cosh\beta - \cos\alpha)^{1/2} \times \sum_{n=0}' A_n e^{-(n+\frac{1}{2})\beta} P_n(\cos\alpha), \quad (4)$$

$$\phi_2 = (\cosh\beta - \cos\alpha)^{1/2} \times \sum_{n=0}' C_n \sinh[(n + \tfrac{1}{2})\beta] P_n(\cos\alpha). \quad (5)$$

The constant coefficients A_n and C_n are to be established with the aid of the matching conditions (3b) at $\beta = \beta_0$.

The requirement of temperature continuity at $\beta = \beta_0$ yields

$$A_n = \frac{a^2\sqrt{2}}{3}(2n + 1)\coth\beta_0 + C_n\sinh[(n + \tfrac{1}{2})\beta_0]\, e^{(n+\frac{1}{2})\beta_0}. \quad (6)$$

The factor $(\cosh\beta - \cos\alpha)^{1/2}$ causes some trouble when we apply the requirement of continuous heat flux at $\beta = \beta_0$ since we cannot equate the resulting series written below on a term by term basis,

$$\sum_{n=0}'' C_n[b_n + d_n\cos\alpha] P_n(\cos\alpha) = \sum_{n=0}'' [h_n + e_n\cos\alpha] P_n(\cos\alpha) \quad (7)$$

where

$$b_n = (n + \tfrac{1}{2})\cosh\beta_0\{\sinh[(n + \tfrac{1}{2})\beta_0] + (k_2/k_1)\cosh[(n + \tfrac{1}{2})\beta_0]\} - \tfrac{1}{2}[1 - (k_2/k_1)]\sinh[(n + \tfrac{1}{2})\beta_0]\sinh\beta_0,$$

$$d_n = -(n + \tfrac{1}{2})\{\sinh[(n + \tfrac{1}{2})\beta_0] + (k_2/k_1)\cosh[(n + \tfrac{1}{2})\beta_0]\},$$

$$h_n = \frac{\sqrt{2}}{3}(2n + 1)e^{-(n+\frac{1}{2})\beta_0}\cosh\beta_0,$$

$$e_n = \frac{-\sqrt{2}}{3}(2n + 1)e^{-(n+\frac{1}{2})\beta_0}.$$

With the aid of the recurrence relation

$$\cos\alpha\, P_n(\cos\alpha) = \left(\frac{n}{2n+1}\right)P_{n-1}(\cos\alpha) + \left(\frac{n+1}{2n+1}\right)P_{n+1}(\cos\alpha), \quad (8)$$

we obtain a set of linear equations for the coefficients C_n

$$C_0b_0 + \frac{1}{3}C_1d_1 = h_0 + \frac{1}{3}e_1,$$

$$\left(\frac{n}{2n-1}\right)C_{n-1}d_{n-1} + C_nb_n + \left(\frac{n+1}{2n+3}\right)C_{n+1}d_{n+1} = \left(\frac{n}{2n-1}\right)e_{n-1} + h_n + \left(\frac{n+1}{2n+3}\right)C_{n+1}, \quad n \geqslant 1. \quad (9)$$

This set of equations cannot be solved since any N equations involve $N + 1$ unknowns. However, since C_n is a decreasing series, it can be truncated at some $n = N$. Should we set $C_{N+1} = 0$, the above equations (7) can be solved in a closed form for any N.

An alternative method of solution can be obtained by constructing an additional equation

$$-2\pi k_2\int_\pi^0\left(r\frac{\partial\phi_2}{\partial\beta}\right)d\alpha = \frac{4}{3}\pi k_1 \quad \text{for any constant } \beta \geqslant \beta_0. \quad (10)$$

The RHS of equation (10) represents the total rate of heat generated in the sphere, while the LHS represents the total rate of heat flow through any β = constant surface enclosing the sphere. Evaluation of the integral in equation (10) leads to the equation

$$\sum_{n=0}^{\infty} C_n = \frac{(\sqrt{2})}{3a}(k_2/k_1). \tag{11}$$

Now if we truncate equations (9) and (11), we obtain a closed set which can be solved for any N.

In the special case of $(k_2/k_1) = 1$, we obtain the closed form solution

$$C_n = \left(\frac{2\sqrt{2}}{3}\right)(k_2/k_1)\, e^{-(2n+1)\beta_0} \quad n = 0, 1, 2, \ldots. \tag{12}$$

For more general circumstances $(k_2/k_1 \neq 1)$, we use a numerical procedure. As mentioned earlier, we can either solve the set (9) alone or solve equations (9) and (11) together. The latter method enjoys quicker convergence but is susceptible to truncation errors. Hence, if great accuracy is desired the first method is preferable.

The numerical technique takes advantage of the fact that the matrix of coefficients in equation (9) is essentially tridiagonal; because of this, we can apply a modified version of the Gauss–Jordan elimination technique, in which a special provision is added to diagonalize equation (11). By doing this, we avoid matrix inversion and save computer storage space (only three coefficients have to be stored for each equation).

As a convergence criteria, we require

$$1 - \frac{\phi_N}{\phi_{N_1}} < \varepsilon, \quad N_1 > N \tag{13}$$

where ϕ_N is obtained by truncating the equations (9) and (11) at some value N. In the calculations presented here, we use $N_1 = N + 5$ and $\varepsilon \leqslant 0.001$. The convergence is fairly rapid. For example, for $\beta_0 = 0.2$ $(D/R = 1.02)$, and for $\beta_0 = 2$ $(D/R = 3.76)$, we need $N = 35$ and $N = 4$, respectively.

The fact that C_N decays exponentially aids in estimating the number N needed to satisfy condition (13). We use equation (5) to evaluate ϕ_2 at point $\alpha = 0$ on the sphere surface $(\beta = \beta_0)$. Next, we replace the sinh term in equation (5) with an exponent. The resulting infinite and truncated series are geometric; consequently they can be summed. Stipulating that $1 - \phi_N/\phi_\infty \leqslant \varepsilon$, we get

$$N \geqslant -\frac{\ln\varepsilon}{\beta_0} \tag{14}$$

which provides an estimate for the number of terms N needed to achieve desired accuracy. Criteria (14) and (13) give comparable results.

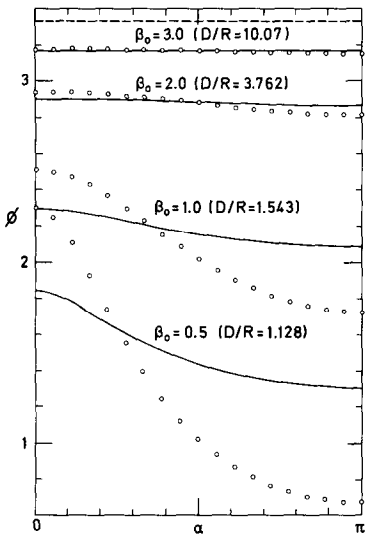

FIG. 2. The temperature distribution on the sphere surface is shown for spheres buried at various depths. The medium-sphere thermal conductivity ratio (k_2/k_1) is 0.1. The solid curves and the circles represent, respectively, exact and approximate results. The dashed line represents a solution for a sphere buried in an infinite medium.

3. THE SOURCE–SINK SOLUTION

A heat source and a heat sink of equal strength are placed at equal distances (D/R) on both sides of the isothermal surface. The temperature distribution is separately calculated for a heat source and a heat sink in an infinite medium, and then the two solutions are superposed. The resulting temperature distribution inside the sphere $(\bar{\phi}_1)$ is

$$\bar{\phi}_1 = \frac{1}{6}(1 - r_1^2) + \frac{1}{3}(k_1/k_2)\left(1 - \frac{1}{r_2}\right) \quad r \leqslant 1 \tag{15}$$

and outside the sphere

$$\bar{\phi}_2 = \frac{1}{3}(k_1/k_2)\left(\frac{1}{r_1} - \frac{1}{r_2}\right) \quad r \geqslant 1 \tag{16}$$

where r_1 and r_2 are the distances from the source and the sink, respectively. In terms of the rectangular coordinates (r, z), r_1 and r_2 can be expressed as

$$r_{1,2} = [(z \pm D/R)^2 + r^2]^{1/2} \tag{17}$$

where the $(-)$ and $(+)$ signs refer to r_1 and r_2, respectively.

Expressions (15) and (16) are exact in the special case of $(k_2/k_1) = 1$. In this case equations (15) and (16) are equivalent to equations (4) and (5). In the more general case of $(k_2/k_1) \neq 1$, equations (15) and (16) provide an approximation whose accuracy improves as the burial depth is increased. The comparison between the exact and approximate results is given in the next section.

4. RESULTS AND DISCUSSION

In this section we present the temperature distribution in and around the sphere (Figs. 2–6), the form factor (Fig. 7), and the heat flux distribution along the surface of the medium (Figs. 8–9) for spheres buried at various depths and for various thermal conductivity ratios (k_2/k_1). The exact solution, presented as a solid line, is compared to the approximate sink–source solution (denoted by circles).

4.1. *Temperature distribution in and around the sphere*

Often, as in the case of nuclear waste burial, one has to verify that the temperatures inside the sphere and on its surface do not exceed certain values. For this purpose knowledge of the temperature field is important.

The temperature distribution around the sphere surface is given in Figs. 2 and 3. Figure 2 shows the effect of the burial depth. As the burial depth increases the surface temperature increases as well, the temperature profile flattens and the deviation between the exact and approximate solutions decreases. For $D/R \geqslant 4$ the deviation is smaller than 2%. For large D/R both solutions resemble those of a sphere buried in an infinite medium, for which $\phi = k_1/3k_2$ (dashed line in Fig. 2).

The effect of the thermal conductivity ratio is examined in Fig. 3 for a sphere buried at depth $D/R = 1.128$ ($\beta_0 = 0.5$). As the ratio k_2/k_1 decreases (the relative conductivity of the sphere increases) the temperature distribution becomes more uniform. An increase in the thermal conductivity of the medium results in lower temperatures at the sphere surface. Roughly speaking, the temperature at the sphere surface is inversely proportional to the ratio k_2/k_1. For the special case of $(k_2/k_1) = 1$, the approximation becomes exact and the circles coincide with the solid lines.

The axial temperature profile inside the sphere is shown in Fig. 4 for various burial depths. The maximum temperature is achieved at a point below the sphere center. As the burial depth increases the temperature inside the sphere becomes more uniform and the apex approaches the sphere center. For small burial depths the approximate solution exhibits nonphysical behavior in which the maximum temperature occurs at the sphere bottom. Similar results are evident in Fig. 5 where the temperature apex relative to the sphere center (the ordinate) is shown as a function of the burial depth. As noted earlier, the temperature apex approaches the sphere center as the burial depth increases. This trend is accelerated as the relative thermal conductivity of the sphere decreases. The magnitude of the maximum temperature is shown in Fig. 6 as a function of the burial depth. The maximum temperature increases with increasing burial depth and approaches asymptotically the corresponding value of a sphere buried in an infinite medium for which $\Phi_{max} = k_1/3k_2 + 1/6$ (dashed line in Fig. 6). The approximate solution is exact for $k_2/k_1 = 1$ and gives good results for $k_2/k_1 \geqslant 1$ even for small burial depths. For $k_2/k_1 < 1$, the approximation is good within 2% for $D/R \geqslant 4$.

4.2. *The form factor*

A form factor (F) for the heat generating sphere can be defined in the following way:

$$F = \frac{Q}{k_2(T_{AV} - T_{SUR})} = \frac{4}{3}(k_1/k_2)\frac{\pi R}{\phi_{AV}}$$

where T_{AV} and T_{SUR} are the dimensional average temperatures of the sphere and the surface, respectively. ϕ_{AV} is the average nondimensional temperature. By integrating equations (4) and (15) over the sphere volume, we obtain the exact average temperature

$$\phi_{AV} = -\frac{1}{15}[3\cosh^2\beta_0 + 1 + 2a^2] + (2a)^{1.2}\sum_{n=0}^{r} A_n e^{-(2n+1)\beta_0}, \quad (18)$$

and the approximate one,

$$\phi_{AV} = \frac{1}{15} + \left(\frac{1}{3} - \frac{1}{6}\frac{R}{D}\right)(k_1/k_2). \quad (19)$$

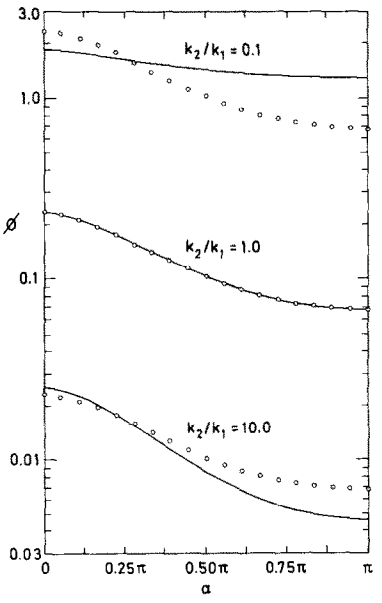

FIG. 3. The temperature distribution on a sphere surface buried at depth $D/R = 1.128$ ($\beta_0 = 0.5$) is shown for various medium-sphere thermal conductivity ratios (k_2/k_1). The solid curves and the circles represent, respectively, exact and approximate results.

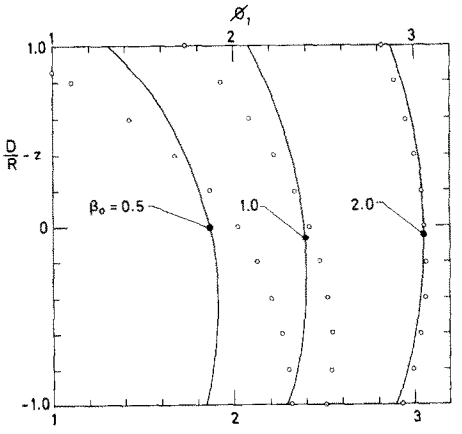

FIG. 4. The axial temperature distribution is shown for various burial depths. The thermal conductivity ratio $k_2/k_1 = 0.1$. The solid lines and the circles represent, respectively, exact and approximate results.

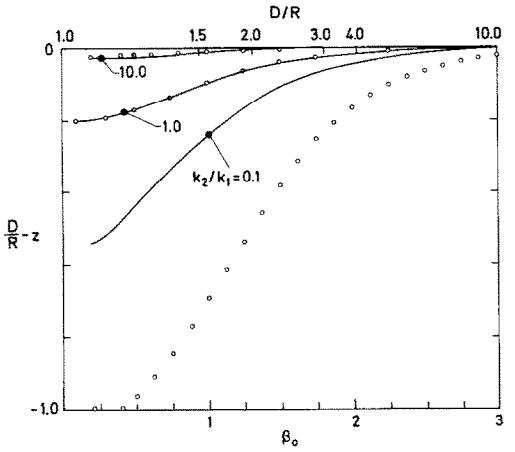

FIG. 5. The location of the maximum temperature inside the sphere as a function of the burial depth (D/R) is shown for various sphere-medium thermal conductivity ratios. The solid lines and the circles represent the exact and approximate solutions, respectively.

It can be easily shown that equations (18) and (19) are identical in the special case of $(k_2/k_1) = 1$.

The average temperature ϕ_{AV} and the form factor F are shown in Fig. 7. The average temperature increases with the burial depth and approaches asymptotically the value of $k_1/3k_2 + 1/15$ (dashed line in Fig. 7). The accuracy of the approximation (19) improves as the burial depth increases. For $D/R \geqslant 2$ the approximation is correct within 2%.

The ordinate of Fig. 7 is inversely proportional to the form factor. We compare our form factors to the one given by Weihs and Small [8] for an isothermal sphere buried beneath an isothermal surface (shown as dash-dot line in Fig. 7). For spheres with high thermal conductivity (small k_2/k_1) their shape factor approaches ours as the burial depth increases. For example, for $(k_2/k_1) = 0.1$ and $D/R > 1.8$, the deviation between their results and ours is smaller than 3%.

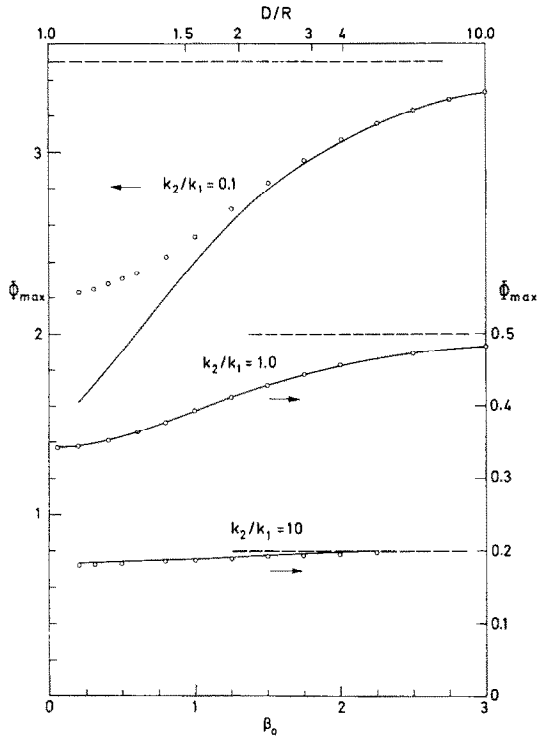

FIG. 6. The maximum temperature inside the sphere as a function of the burial depth (D/R) is shown for various sphere-medium thermal conductivity ratios. The solid lines and the circles represent the exact and approximate solutions, respectively. The dashed lines are asymptotic solutions for spheres buried in an infinite medium.

4.3. *The heat flux distribution at the medium surface*

The heat flux distribution at the solid surface $(\beta = 0)$ is presented in Figs. 8 and 9. In both figures the ordinate is the nondimensional heat flux q, and the abscissa is the coordinate α. The heat flux is scaled by the group gR. The exact value for the nondimensional heat flux (q) at the surface is calculated from

$$q = \frac{k_2}{k_1}\left(\frac{\cosh\beta - \cos\alpha}{a}\frac{\partial\phi_2}{\partial\beta}\right)_{\beta=0}, \qquad (20)$$

and the approximate value for the heat flux $(\bar{q})$ is

$$\bar{q} = \frac{k_2}{k_1}\left(\frac{\partial\bar{\phi}_2}{\partial z}\right)_{z=0} = \frac{2}{3}\frac{D/R}{[(D/R)^2 + r^2]^{3/2}}. \qquad (21)$$

Again the source–sink solution (21) is exact in the special case of $(k_2/k_1) = 1$. The effect of the thermal conductivity ratio k_2/k_1 on the heat flux distribution along the solid surface is demonstrated in Fig. 8. The approximate heat flux distribution $[\bar{q}$, equation (21)] is independent of the ratio k_2/k_1. In contrast, the exact heat flux distribution along the solid surface varies with k_2/k_1. As the ratio k_2/k_1 decreases, greater amounts of heat are released immediately above the sphere. The sphere cross-section is shown schematically in the right hand corner of Fig. 8.

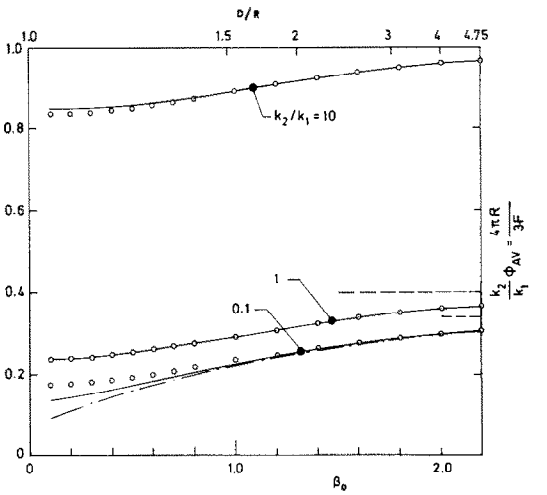

FIG. 7. The average temperature inside the sphere and the form factor (F) are shown as a function of the burial depth (D/R). The solid lines and the circles represent the exact and approximate solutions, respectively. The dotted line is the form factor from ref. [8] for an isothermal sphere.

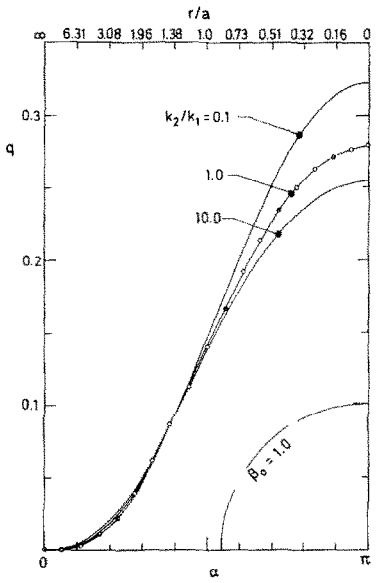

FIG. 8. The heat flux along the medium surface resulting from a sphere buried at depth $D/R = 1.543$ ($\beta_0 = 1.0$) is shown for various medium-sphere thermal conductivity ratios (k_2/k_1). The solid curves and the circles represent exact and approximate results, respectively.

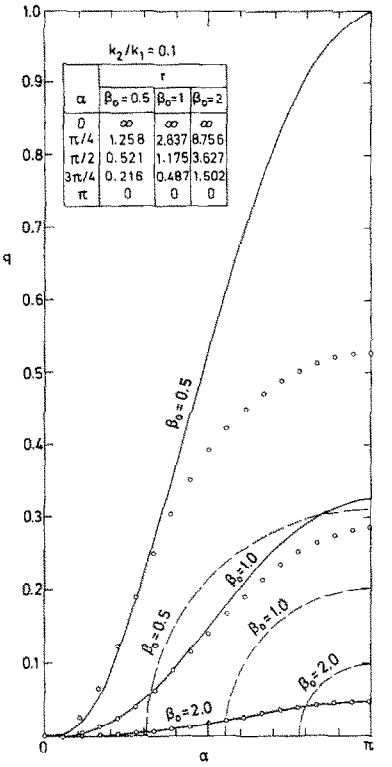

FIG. 9. The heat flux distribution along the medium surface is shown for spheres buried at various depths. The medium-sphere thermal conductivity ratio is 0.1.

In Fig. 9, the effect of the burial depth (D/R) on the heat flux distribution (q) at the surface ($\beta = 0$) is examined. The abscissa (α) is somewhat misleading, since the same values of α correspond to different horizontal distances (r) for the different curves. To facilitate comparison, the projection of the sphere (same size in all cases) is presented with a broken line in the right hand corner of Fig. 9. Also, a table is presented at the top of the left side translating a few α values into r values for the different cases. As the depth of the sphere center (D/R) increases, the heat flux is distributed on a larger area, and the peak at the sphere axis decreases. Also, as the burial depth increases, the approximate solution (21) approaches the exact one (20).

5. CONCLUSION

Procedures for obtaining exact and approximate temperature distributions in and around a heat generating buried sphere have been presented. The exact solution was obtained using a bispherical coordinate system. The source–sink solution provides exact results for the special case when the thermal conductivities of the sphere and the medium equal each other and serves as an approximation in all other cases. The approximations for the temperature field and for the form factor are correct within 2% for $D \geq 4R$ and $D \geq 2R$, respectively.

Acknowledgements—I thank Professor Sadhal for useful discussions and the Department of Mechanical Engineering and Applied Mechanics of the University of Pennsylvania for financial support.

REFERENCES

1. H. S. Carslaw and J. C. Jaeger, *Conduction of Heat in Solids* 273 pp. Oxford University Press, London (1959).
2. S. S. Attwood, *Electric and Magnetic Fields*, p. 123. Wiley, New York (1932).
3. E. Hahne and U. Grigull, A shape factor scheme for point source configurations, *Int. J. Heat Mass Transfer* **17**, 267–273 (1974).
4. N. N. Lebedev, *Special Functions and their Applications*, p. 230. Dover, New York (1972).
5. P. M. Morse and H. Feshbach, *Methods of Theoretical Physics*, pp. 1298–1304. McGraw–Hill, New York (1953).
6. M. M. Yovanovich, *Advanced Heat Conduction*, unpublished (1969).
7. R. D. Small and D. Weihs, Thermal traces of a buried heat source, *Trans. Am. Soc. Mech. Engrs*, Series C, *J. Heat Transfer* **99**, 47–52 (1977).
8. D. Weihs and R. D. Small, The temperature field in the vicinity of a spherical inclusion, *6th Int. Heat Transfer Conf.*, Vol. 3, pp. 285–290 (1978).

DISTRIBUTION DE TEMPERATURE DANS ET AUTOUR D'UNE SPHERE ENTERREE ET THERMOGENE

Résumé—On présente une solution analytique exacte pour la distribution stationnaire de température dans et autour d'une sphère source de chaleur enterrée dans un solide semi-infini avec une surface isotherme. Cette analyse ne demande pas que les conductivités thermiques du milieu et de la sphère soient égales. La solution exacte obtenue en utilisant un système de coordonnées bisphériques est comparée avec une solution approchée de puit-source. Les résultats incluent la distribution de température dans et autour de la sphère, le facteur de forme et la distribution du flux de chaleur sur la surface libre.

TEMPERATURVERTEILUNG INNERHALB UND IN DER UMGEBUNG EINER EINGEGRABENEN WÄRMEERZEUGENDEN KUGEL

Zusammenfassung—Es wird eine exakte analytische Lösung für die stationäre Temperaturverteilung innerhalb und in der Umgebung einer wärmeerzeugenden Kugel angegeben, die von einem halbunendlichen Feststoff mit einer isothermen Oberfläche unschlossen ist. Die Ableitung erfordert nicht, daß die thermische Leitfähigkeit des Mediums und der Kugel gleich sein müssen. Die exakte Lösung, die unter Verwendung eines bisphärischen Koordinatensystems abgeleitet wurde, wird mit einer näherungsweisen Quellen-Senken-Lösung verglichen. Die Ergebnisse enthalten die Temperaturverteilung innerhalb und in der Umgebung der Kugel, den Formfaktor und die Wärmestromdichten-Verteilung an der Oberfläche des Mediums.

РАСПРЕДЕЛЕНИЕ ТЕМПЕРАТУР ВНУТРИ И ВОКРУГ ПОГРУЖЕННОГО ТЕПЛОВЫДЕЛЯЮЩЕГО СФЕРИЧЕСКОГО ТЕЛА

Аннотация—Дано точное аналитическое решение для стационарного распределения температур внутри и вокруг тепловыделяющего сферического тела, помещенного внутрь полубесконечного твердого тела с изотермической поверхностью. Равенство теплопроводностей двух тел не предполагается. Проведено сравнение точного решения, полученного с помощью бисферической системы координат, с приближенным решением по методу "источник-сток". Определены профили температур внутри и вокруг сферического тела, форм-фактор и распределение плотности теплового потока по поверхности твердого тела.